# Correlations in orbital angular momentum of spatially entangled paired photons generated in parametric down-conversion

Clara I. Osorio,[1] Gabriel Molina-Terriza,[1,2] and Juan P. Torres[1,3,*]

[1]*ICFO-Institut de Ciencies Fotoniques, Mediterranean Technology Park, 08860 Castelldefels (Barcelona), Spain*
[2]*ICREA-Institucio Catalana de Recerca i Estudis Avancats, 08010 Barcelona, Spain*
[3]*Department of Signal Theory and Communications, Universitat Politecnica de Catalunya, Campus Nord, 08034 Barcelona, Spain*
(Received 22 May 2007; published 25 January 2008)

What are the orbital angular momentum correlations between spatially entangled photon pairs generated in spontaneous parametric down-conversion? We show that the answer to this question can be given in two alternative, although complementary, ways. The answer posed in this Brief Report explains satisfactorily the *seemingly contradictory* results obtained in different experiments, and theoretical approaches.

Within the paraxial quantum optics regime, the orbital angular momentum (OAM) provides a useful description of the spatial degree of freedom of photons. Photons whose spatial waveform contains an azimuthal phase dependence of the form $\sim \exp(im\varphi)$, carry an OAM of $m\hbar$ per photon [1]. Photons with diverse spatial waveforms can be easily generated, detected, and controlled. Therefore the OAM offers a physical resource to explore deeper quantum features not present in the two-dimensional (2D) Hilbert space addressed when using the polarization [2,3]. Indeed, it allows us to readily tailor the number of effective dimensions of the Hilbert space [4].

During the last few years, several quantum features based on the capacity of the OAM of photons to go beyond a 2D Hilbert space have been demonstrated (see [5] and references inside) using spontaneous parametric down-conversion (SPDC). These include the demonstration of the violation of bipartite, three-dimensional Bell inequalities [6], the implementation of the so called *quantum coin tossing* protocol with qutrits [7], and the generation of quantum states in ultrahigh dimensional spaces [8].

All of these experiments make use of the existence of specific quantum OAM correlations between the two entangled photons generated in the SPDC process. Several experiments [2,9–11] seem to support the validity of the selection rule $m_p = m_1 + m_2$, where $m_p\hbar$ is the OAM per photon of the classical pump beam, and $m_1$ and $m_2$ are the winding numbers of the modes into which the quantum state of the signal and idler photons are projected, respectively. Some other experiments [12–14], while not directly measuring the OAM of the down-converted photons, demonstrate the existence of ellipticity of the spatial wave form, which should make possible the detection of photons with $m_p \neq m_1 + m_2$. Under some restrictive conditions, the selection rule $m_p = m_1 + m_2$ can be derived from first principles [4,15,16], although, as it will be shown below, the same rule addresses different physical quantities. The presence of Poynting vector walk-off can also strongly modify OAM correlations [17].

All this raises the question of what are the OAM correlations between the down-converted photons generated in SPDC, i.e., under which conditions the OAM of the entangled photons fulfill the selection rule $m_p = m_1 + m_2$. Here we show that this question can be formulated in two complementary scenarios, so that in each scenario the sought-after OAM correlations can be different. The existence of previous *apparently contradictory* results is due to the fact that the sought-after OAM correlations are different.

In one scenario, the spatial properties of all the pairs of photons generated are considered, therefore the *global* mode function is obtained adding coherently all such possibilities. In another scenario, which is relevant for current experimental applications, a small section of the full down-conversion cone is considered. Only certain probability amplitudes are now considered. Under these conditions, the noncollinear SPDC geometry and the presence of spatial walk-off can greatly modify the OAM correlations observed.

We consider a nonlinear crystal of length $L$, illuminated by a monochromatic laser pump beam propagating in the $z$ direction, with frequency $\omega_p$. The spatial shape of the pump beam at the center of the nonlinear crystal ($z=L/2$), in the transverse wave-vector domain, writes $E_p^+(\bar{\mathbf{p}}) = E_0(\bar{p}_x + i\bar{p}_y)^{m_p} \exp(-|\bar{\mathbf{p}}|^2 w_0^2/4)$, which corresponds to a beam which carries an OAM of $m_p\hbar$ per photon. $E_0$ is a normalizing constant, $\bar{\mathbf{p}} = (\bar{p}_x, \bar{p}_y)$ is the transverse wave vector, and $w_0$ is the beam width. The signal and idler photons are assumed to be monochromatic, with $\omega_s = \omega_i = \omega_p/2$, where $\omega_{s,i}$ are the frequencies of the signal and idler photons. This is justified by the use of narrow-band interference filters in front of the detectors.

The photons are known to be generated into cones, whose shape is determined by the phase matching conditions inside the crystal. For the sake of clarity, let us consider first noncritical, i.e., negligible walk-off, noncollinear SPDC in a periodically poled nonlinear crystal. The angle of the down-conversion cone is assumed to be small, so that the polarization [18] and refractive index do not show noticeable changes with the direction of propagation. Similarly, the nonlinear coefficient is assumed to be constant along the down-conversion cone.

The SPDC process can be described in the interaction picture by an effective Hamiltonian given by [19] $H_I = \epsilon_0 \int_V dV \chi^{(2)} E_p^+ E_s^- E_i^- + \text{c.c.}$, where $E_s^-(\mathbf{x}, z, t)$

*juan.perez@icfo.es

$\propto \int dK_s d\mathbf{P} \exp(-i\mathbf{P}\cdot\mathbf{x}-iK_s z+i\omega_s t)a^\dagger(K_s,\mathbf{P})$ refers to the negative-frequency part of the signal electric field operators, and similarly for the idler photon. The two-photon quantum state $|\Psi\rangle$, within the first order perturbation theory, can be written as $|\Psi\rangle=\int d\mathbf{P}d\mathbf{Q}\Phi(\mathbf{P},\mathbf{Q})a_s^\dagger(\mathbf{P})a_i^\dagger(\mathbf{Q})|0,0\rangle$, where $\mathbf{P}$ and $\mathbf{Q}$ are the transverse wave vector for the signal and the idler, respectively, and the mode function $\Phi$ is given by

$$\Phi(\mathbf{P},\mathbf{Q}) = E_p(\mathbf{P}+\mathbf{Q})\mathrm{sinc}\left(\frac{\Delta_k L}{2}\right) \quad (1)$$

where $\Delta_k = K_p(\mathbf{P}+\mathbf{Q})-K_s(\mathbf{P})-K_i(\mathbf{Q})$, the wave vectors $(j=s,i,p)$ write $K_j(\mathbf{P})=[(\omega_j n_j/c)^2-|\mathbf{P}|^2]^{1/2}$, depends on the modulus of the corresponding transverse wave vectors, and $n_j$ are the corresponding refractive index. The mode function of the biphoton in the spatial domain $(\mathbf{x}_1,\mathbf{x}_2)$ is the spatial Fourier transform of the mode function given by Eq. (1).

We can write $|\mathbf{P}+\mathbf{Q}|^2=\rho_s^2+\rho_i^2+2\rho_s\rho_i\cos(\varphi_s-\varphi_i)$, where $\rho_s=|\mathbf{P}|$, and $\varphi_s=\tan^{-1}P_y/P_x$ are the modulus and phase of the transverse wave vector $\mathbf{P}$ in cylindrical coordinates. For the idler photon we have, similarly, $\rho_i=|\mathbf{Q}|$ and $\varphi_i=\tan^{-1}Q_y/Q_x$. One can write $\mathrm{sinc}(\Delta_k L/2)=\sum_{l=-\infty}^{\infty}\mathcal{H}_l(\rho_s,\rho_i)\exp\{il(\varphi_s-\varphi_i)\}$. $K_{s,i}$ depends on the moduli $\rho_{s,i}$, respectively. The pump beam can also be written as

$$E_p = E_0 \exp\left\{-\frac{[\rho_s^2+\rho_i^2+\rho_s\rho_i\cos(\varphi_s-\varphi_i)]w_0^2}{4}\right\}$$
$$\times \sum_{l=0}^{m_p}\binom{m_p}{l}\rho_s^l\rho_i^{m_p-l}\exp\{il\varphi_s+i(m_p-l)\varphi_i\}. \quad (2)$$

Therefore the mode function given by Eq. (1) can be written as

$$\Phi(\mathbf{P},\mathbf{Q}) = \sum_{m=-\infty}^{\infty}\mathcal{G}_m(\rho_s,\rho_i)\exp[im\varphi_s+i(m_p-m)\varphi_i]. \quad (3)$$

The main conclusion to be drawn from Eq. (3) is that if polarization, refractive index, and nonlinear coefficient show negligible azimuthal variations around the down-conversion cone, the OAM correlations of the spatial waveform of the biphoton state fulfill $m_p=m_1+m_2$ [15]. Importantly, this result requires considering *the whole spatial waveform of the down-converted photons, i.e., the full down-conversion cone*. Notwithstanding, these *are not* the OAM correlations that typical quantum information experiments based on spatial entanglement measure. An experiment aimed at detecting the *global* OAM of the down-converted photons is a significant experimental challenge that it is yet to be solved.

All relevant experiments reported to date detect only a small section of the full down-conversion cone. In other words, the wave vectors of the signal and idler photons belong to a narrow bundle around the corresponding central wave vectors, i.e., $\mathbf{P}=\mathbf{P}_0+\Delta\mathbf{P}$ and $\mathbf{Q}=\mathbf{Q}_0+\Delta\mathbf{Q}$. As shown in Fig. 1, the signal photon propagates along the direction $\hat{z}_1$ with longitudinal wave vector $k_s(\mathbf{p})=[(w_s n_s/c)2-|\mathbf{p}|^2]^{1/2}$, and transverse wave vector $\mathbf{p}=(p_x,p_y)$, so that $\Delta P_x=p_x$ and $\Delta P_y=\cos\theta_1 p_y-\sin\theta_1 k_s$. And similarly for the idler photon, which propagates in the direction $\hat{z}_2$ with longitudinal wave
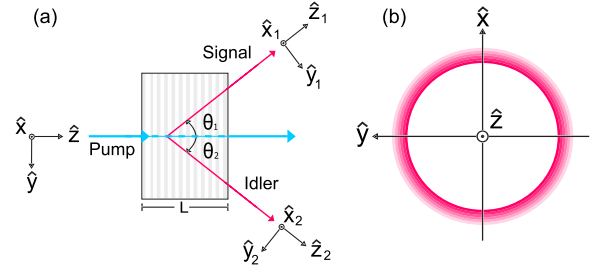


FIG. 1. (Color online) Schematic diagram of a noncollinear SPDC. (a) Top view of the noncollinear configuration. (b) The down-conversion cone.

vector $k_i(\mathbf{q})$ and transverse wave vector $\mathbf{q}$, so that $\Delta Q_x=q_x$ and $\Delta Q_y=\cos\theta_2 q_y-\sin\theta_2 k_i$. We restrict ourselves to the case $\theta_1=-\theta_2=\theta$.

The quantum state of the biphoton at $z_1=L/\cos\theta$ can be written as $|\psi\rangle=\int d\mathbf{p}d\mathbf{q}\Phi(\mathbf{p},\mathbf{q})a_s^+(\mathbf{p})a_i^+(\mathbf{q})|0,0\rangle$, where the mode function writes [20]

$$\Phi(\mathbf{p},\mathbf{q}) = E_p(p_x+q_x,\delta_0)\mathrm{sinc}\left(\frac{\delta_k L}{2}\right) \quad (4)$$

where $\delta_k=k_p-(k_s+k_i)\cos\theta-(p_y-q_y)\sin\theta$ and $\delta_0=(p_y+q_y)\cos\theta-(k_s+k_i)\sin\theta$.

The mode function given by Eq. (4) shows ellipticity in the $(\mathbf{p},\mathbf{q})$ domain, as has been demonstrated experimentally [12,14]. An increasing degree of ellipticity of the spatial mode function enhances the quantum probability amplitude of paired photons with $m_p\neq m_1+m_2$. To get further insight in the nature of the OAM correlations, let us consider that the idler photon is projected into a gaussian mode $(m_2=0)$, so that the quantum state of the signal photon is described by the reduced mode function $\Phi_s(\mathbf{p})\propto\int d\mathbf{q}\Phi(\mathbf{p},\mathbf{q})\exp(-|\mathbf{q}|^2 w_1^2/4)$, where $w_1$ is the beam width of the idler mode at the center of the nonlinear crystal. To elucidate the OAM content of the signal photon, one has to project the spatial mode function into spiral harmonics $\exp(im\varphi)$. The weights for each $m$ of such decomposition gives us the sought-after OAM decomposition [3].

Figure 2(a) shows the total weight corresponding to OAM modes with $m_1\neq 0$, which is a measure of the degree of violation of the selection rule $m_p=m_1+m_2$, for different values of the noncollinear angle and the pump beam width. Notice that the larger the noncollinear angle $\theta$, and the smaller the pump beam width $w_0$, the larger is the probability to detect signal photons with $m_1\neq 0$. Figures 2(b) and 2(c) show two OAM distributions for $\theta=5°$, one which shows an OAM distribution with modes with $m_1\neq 0$, while the other shows a single peak for $m_1=0$.

The strength of the violation of the selection rule $m_p=m_1+m_2$ can be quantified through the noncollinear length [17] $L_{nc}=w_0/\sin\varphi$. If the crystal length is much smaller than the noncollinear length $(L\ll L_{nc})$, the ellipticity of the mode function is small, and thus the selection rule $m_p=m_1+m_2$ is fulfilled. This turns out to be the case of nearly all of the experiments that make use of the OAM of photons [2,6–11]. Typical noncollinear angles and crystal lengths used in these
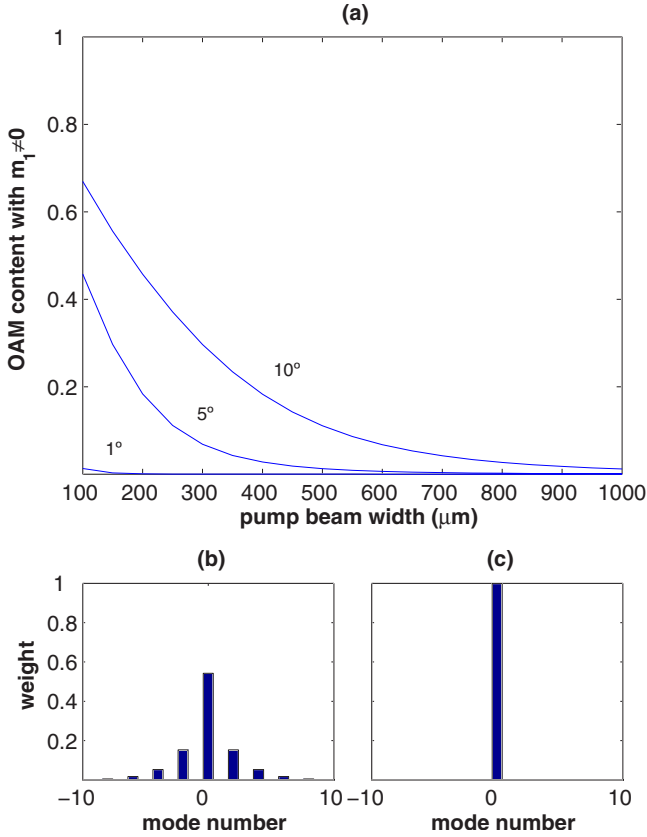
FIG. 2. (Color online) Orbital angular momentum of the signal photon in noncollinear SPDC in a $L=10$ mm long PPKTP crystal. The pump beam is Gaussian ($m_p=0$). Both photons traverse $2f$ systems. The idler photon is detected with $\mathbf{q}=\mathbf{0}$, which corresponds to $w_1 \rightarrow \infty$. (a) Total weight of the OAM modes with $m_1 \neq 0$, as a function of the pump beam width ($w_0$). The label designates the noncollinear angle. (b), (c) OAM mode distribution for $\theta=5°$ for two values of the pump beam width: $w_0=100$ $\mu$m and $w_0 = 1000$ $\mu$m.

experiments are $\theta \simeq 1-2°$ and $L \simeq 1-5$ mm. For $w_0 = 500$ $\mu$m, one obtains $L_{nc} \simeq 15-30$ mm, so that $L < L_{nc}$. On the contrary, if $L \gtrsim L_{nc}$, strong departures from the selection rule $m_p = m_1 + m_2$ are expected. This is the experimental configuration in [12–14], due to the use of a highly focused pump beam or longer crystals. For $w_0=90$ $\mu$m and $\theta=2°$, one has $L_{nc} \simeq 2.5$ mm.

According to Eq. (3), the OAM of the spatially entangled photons fulfill the relationship $m_p = m_1 + m_2$, while Fig. 2 shows that strong departures from this selection rule can be observed if highly focused pump beams, highly noncollinear configurations, or longer nonlinear crystals are used. Actually, *we are describing the same quantum process in two complementary scenarios*. Figure 2 would give us the OAM correlations measured in typical experiments that use the OAM as a physical resource for quantum information, thus it is relevant for experimental configurations currently used. In this scenario, the fulfillment of the condition $m_p = m_1 + m_2$ depends on the pump beam width and the noncollinear angle, as dictated by the interplay between the noncollinear and crystal lengths.

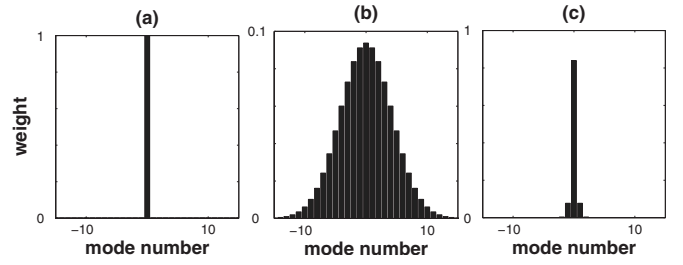On the other hand, Eq. (3) corresponds to a global view of



FIG. 3. Orbital angular momentum distribution of the pump beam in different positions inside the nonlinear crystal. (a) $z=0$, (b) $z=5$ mm and $w_0=100$ $\mu$m, and (c) $z=5$ mm and $w_0=1$ mm. The walk-off angle is $\rho_0=5°$.

the SPDC process, where the full down-conversion cone is considered. The question of angular momentum conservation balance in SPDC requires the simultaneous consideration of the angular momentum of the electronic spins and orbitals, the crystalline structure of the nonlinear crystal, and of the electromagnetic field [21]. The analysis presented here might be an important step towards clarifying how angular momentum is effectively conserved, since to evaluate conservation laws, one should take into account *all probability amplitudes* that contribute to the quantum process.

Another important effect that might modify the OAM correlations is the presence of Poynting vector walk-off in some, or all, of the interacting waves. In type I and type II SPDC configurations, some of the interacting waves are extraordinary waves, thus show Poynting vector walk-off. For the sake of simplicity, let us consider a type I configuration, where only the pump beam presents spatial walk-off. An initially gaussian pump beam, at each position $z$ inside the nonlinear crystal, can be decomposed into spiral harmonics as

$$E_p(\rho_{\mathbf{p}}, z) = E_0 \exp\left\{ -\rho_p^2 \left( \frac{w_0^2}{4} + i \frac{z}{2k_p^0} \right) \right\}$$
$$\times \sum_{n=-\infty}^{\infty} J_n(z\rho_p \tan \rho_0) \exp\{in\varphi_p\}, \quad (5)$$

where $\rho_0$ is the spatial walk-off angle, $\varphi_p$ is the azimuthal angle in cylindrical coordinates and $J_n$ are Bessel functions of the first kind, and $k_p^0$ is the longitudinal wave vector. As shown in Fig. 3, the OAM distribution of the pump beam increases its width with distance $z$. A gaussian beam incident from air into the nonlinear crystal is no longer a Gaussian beam, i.e., the pump beam is no longer a wave with $m_p=0$.

This effect becomes noticeable only if $L > L_w$, where the walk length writes $L_w = w_0 / \tan \rho_0$. Figure 3(a) shows the initial OAM distribution of a Gaussian beam, which corresponds to a single peak with $m_p=0$. Figures 3(b) and 3(c) show the OAM distribution at $L=5$ mm for a walk-off angle of $\rho_0=5°$. For highly focused pump beams, the walk-off length can become smaller than the crystal length, thus the OAM distribution no longer shows a single peak, as shown in Fig. 3(b). In this case, $L_w \simeq 1$ mm. The walk-off effect might be negligible for larger beam widths, as one can see in Fig. 3(c). Now, one obtains $L_w \simeq 12$ mm.

In the walking SPDC consider the spatial waveform of the two-photon can be written as

$$\Phi(\mathbf{P},\mathbf{Q}) = E_p(\mathbf{P}+\mathbf{Q})\text{sinc}(\Delta_k L/2) \qquad (6)$$

where $\Delta_k = k_p(\mathbf{P}+\mathbf{Q}) + (P_x+Q_x)\tan\rho_0 - k_s(\mathbf{P}) - k_i(\mathbf{Q})$. The phase matching function no longer depends on $\varphi_s - \varphi_i$ due to the presence of the spatial walk-off.

The mode function of the two-photon state is a coherent sum of all the partial amplitudes due to the possible generation of a pair of photons at position $z$ inside the crystal [22]. Since the beam moves in the $xz$ plane with angle $\rho_0$ when propagating along $z$, the amplitude for each $z$ shows increasing ellipticity, contributing differently to the total OAM decomposition of the spatial waveform of the two-photon state.

In conclusion, we have shown that the elucidation of the OAM correlations of entangled photons generated in SPDC can be addressed in two complementary scenarios, giving correspondingly different OAM correlations between the photons. One scenario considers the quantum amplitudes in the whole down-conversion cone, while the other scenario, experimentally relevant for quantum information protocols that make use of the OAM, pays attention to a small section of the down-conversion cone.

The results obtained here are of great importance for other configurations where entangled paired photons are generated. This is the case of pairs of photons generated through two-photon Raman transitions in electromagnetic induced transparency schemes [23]. Recently, the OAM correlations between stokes and antistokes photons have been measured in trapped rubidium cold atoms in a counterpropagating nearly collinear geometry [24]. The measured correlations comply with the selection rule $m_p - m_c = m_1 - m_2$, where $m_c$ refers to the OAM per photon of a laser control beam that counterpropagates with the pump beam. The corresponding selection rule for counterpropagating signal and idler photons [20] in SPDC would be $m_p = m_1 - m_2$. We expect that a similar experiment in a highly noncollinear geometry, such as a transverse emitting configuration [25], would yield strong departures from the selection rule $m_p - m_c = m_1 - m_2$ measured for a nearly collinear geometry.

[1] L. Allen, M. W. Beijersbergen, R. J. C. Spreeuw, and J. P. Woerdman, Phys. Rev. A **45**, 8185 (1992).
[2] A. Mair, A. Vaziri, G. Weihs, and A. Zeilinger, Nature (London) **412**, 313 (2001).
[3] G. Molina-Terriza, Juan P. Torres, and L. Torner, Phys. Rev. Lett. **88**, 013601 (2001).
[4] J. P. Torres, A. Alexandrescu, and L. Torner, Phys. Rev. A **68**, 050301(R) (2003).
[5] G. Molina-Terriza, J. P. Torres, and L. Torner, Nat. Phys. **3**, 305 (2007).
[6] A. Vaziri, G. Weihs, and A. Zeilinger, Phys. Rev. Lett. **89**, 240401 (2002).
[7] G. Molina-Terriza, A. Vaziri, R. Ursin, and A. Zeilinger, Phys. Rev. Lett. **94**, 040501 (2005).
[8] J. T. Barreiro, N. K. Langford, N. A. Peters, and P. G. Kwiat, Phys. Rev. Lett. **95**, 260501 (2005).
[9] S. P. Walborn, A. N. de Oliveira, R. S. Thebaldi, and C. H. Monken, Phys. Rev. A **69**, 023811 (2004).
[10] G. Molina-Terriza, A. Vaziri, J. Rehacek, Z. Hradil, and A. Zeilinger, Phys. Rev. Lett. **92**, 167903 (2004).
[11] N. K. Langford *et al.*, Phys. Rev. Lett. **93**, 053601 (2004).
[12] A. R. Altman, K. G. Koprulu, E. Corndorf, P. Kumar, and G. A. Barbosa, Phys. Rev. Lett. **94**, 123601 (2005).
[13] D. C. Burnham and D. L. Weinberg, Phys. Rev. Lett. **25**, 84 (1970).
[14] G. Molina-Terriza, S. Minardi, Y. Deyanova, C. I. Osorio, M. Hendrych, and J. P. Torres, Phys. Rev. A **72**, 065802 (2005).
[15] H. H. Arnaut and G. A. Barbosa, Phys. Rev. Lett. **85**, 286 (2000).
[16] S. Franke-Arnold, S. M. Barnett, M. J. Padgett, and L. Allen, Phys. Rev. A **65**, 033823 (2002).
[17] J. P. Torres, G. Molina-Terriza, and L. Torner, J. Opt. B: Quantum Semiclassical Opt. **7**, 235 (2005).
[18] A. Migdall, J. Opt. Soc. Am. B **14**, 1093 (1997).
[19] D. N. Klyshko, Sov. Phys. JETP **28**, 522 (1969) [Zh. Eksp. Teor. Fiz. **55**, 1006 (1968)].
[20] J. P. Torres, C. I. Osorio, and L. Torner, Opt. Lett. **29**, 1939 (2004).
[21] N. Bloembergen, in *Polarization, Matiere et Rayonnement* (Presses Universitaires, Paris, 1969), p. 109.
[22] M. H. Rubin, D. N. Klyshko, Y. H. Shih, and A. V. Sergienko, Phys. Rev. A **50**, 5122 (1994).
[23] V. Balić, D. A. Braje, P. Kolchin, G. Y. Yin, and S. E. Harris, Phys. Rev. Lett. **94**, 183601 (2005).
[24] R. Inoue *et al.*, Phys. Rev. A **74**, 053809 (2006).
[25] P. Kolchin, S. Du, C. Belthangady, G. Y. Yin, and S. E. Harris, Phys. Rev. Lett. **97**, 113602 (2006).